

CNNs-based Acoustic Scene Classification using Multi-Spectrogram Fusion and Label Expansions

Weiping Zheng¹, Zhenyao Mo¹, Xiaotao Xing¹, and Gansen Zhao¹

¹School of Computer, South China Normal University,
Guangzhou 510631, China

(e-mail: zhengweiping@m.scnu.edu.cn; mozhenyaomyz@163.com;
20142100007@m.scnu.edu.cn; gzhao@m.scnu.edu.cn)

Spectrograms have been widely used in Convolutional Neural Networks based schemes for acoustic scene classification, such as the STFT spectrogram and the MFCC spectrogram, etc. They have different time-frequency characteristics, contributing to their own advantages and disadvantages in recognizing acoustic scenes. In this letter, a novel multi-spectrogram fusion framework is proposed, making the spectrograms complement each other. In the framework, a single CNN architecture is applied onto multiple spectrograms for feature extraction. The deep features extracted from multiple spectrograms are then fused to discriminate the acoustic scenes. Moreover, motivated by the inter-class similarities in acoustic scene datasets, a label expansion method is further proposed in which super-class labels are constructed upon the original classes. On the help of the expanded labels, the CNN models are transformed into the multitask learning form to improve the acoustic scene classification by appending the auxiliary task of super-class classification. To verify the effectiveness of the proposed methods, intensive experiments have been performed on the DCASE2017 and the LITIS Rouen datasets. Experimental results show that the proposed method can achieve promising accuracies on both datasets. Specifically, accuracies of 0.9744, 0.8865 and 0.7778 are obtained for the LITIS Rouen dataset, the DCASE Development set and Evaluation set respectively.

Index Terms—Acoustic Scene Classification, Convolutional Neural Networks, Label Expansion, Multitask Learning, Multi-spectrogram.

I. INTRODUCTION

ACOUSTIC scene classification (ASC) [1] has shown huge potentials in many industrial and business applications. It has gained increasing attentions in these years. Recently, many convolutional neural networks (CNNs) based solutions have been proposed for acoustic scene classification [2]. They have shown promising performances. Hamid et al. [3] proposed a hybrid approach using deep CNN and binaural i-vectors [4]. This work ranked first in the DCASE2016 challenge. Soo et al. [5] presented a structure composed of parallel LSTM [6] and CNN networks which aimed to extract both sequential and spectro-temporal locality information. Using the similar combined structure with [5] as the feature extractor, Seongkyu et al. [7] proposed a GAN-based [8] data augmentation method for ASC and won the first prize in the DCASE2017 challenge.

In the existing works, CNNs are often combined with other deep networks (such as LSTM [5], GRNN [9], [10]) or traditional features (such as i-vector [3]). In this letter, we propose a multi-spectrogram fusion framework using a single CNN architecture. The CNN network is applied onto multiple spectrograms for feature extraction, resulting in a simple system architecture. Experiments have demonstrated satisfactory results of the proposed methods. On the other hand, inter-class similarity is getting more prominent in ASC. Scene labels are commonly notated according to the functions of the surrounding spaces where the audio segments are

recorded. As a result, there are audio segments which are very similar in acoustic properties while assigned as different scenes, for example, the audio segments of the libraries and that of the bookstores. However, they are simply considered as different classes in the training process. Ignoring their similarities in acoustic properties will probably prevent the deep networks from learning more essential acoustic features. To distinguish the degrees of similarities among classes, a common solution is to use triple loss [11] or quadruplet loss [12] where the hierarchical relations among classes should be carefully organized. Nevertheless, the selections of good anchor points in this method are challenging. Moreover, it requires more training samples and results in a more complex optimization. Multitask learning is another solution, which requires hierarchical labels. However, most acoustic scene datasets merely provide one-level labels.

Motivated by above observations, we build up a multi-spectrogram fusion framework where a single CNN is used for feature extraction. Under this framework, we further propose a label expansion method by constructing super-class labels upon the original classes. Using the expanded labels, the building block CNN is modified into multitask learning form accordingly to exploit the inter-class similarities mentioned above. To the best of our knowledge, constructing labels purposely and integrating them into multitask learning to boosting the classification performance have not yet been explored in ASC.

In this letter, we produce multiple spectrograms for a single audio segment using different signal processing methods. Specifically, we use the STFT [13], CQT [14], and MFCC [15] spectrograms. The combination of STFT and

This work was partially supported by the Guangdong Provincial Scientific and Technological Projects of China under Grant 2016B010109005 and the Characteristic Innovation Projects of the Educational Commission of Guangdong Province, China under Grant 2016KTSCX025.

CQT spectrograms in the fusion scheme has achieved the best performances. We further propose a novel CNN architecture which is trained on these spectrograms respectively. As a result, multiple basic CNN-based models are obtained. These models serve as feature extractors in this fusion scheme. To train the CNN models, spectrograms are split into multiple samples. The samples originated from the same audio segment are fed into a basic model for feature extraction. The extracted deep features are then concatenated using a random sequence. Furthermore, the dimensionality of concatenated feature is reduced by PCA. The resultant feature is called a "global feature" of the audio segment. Corresponding to multiple basic models, multiple global features can be generated for an audio segment. They are further concatenated into an "aggregated feature". Using aggregated features of the audio segments in the training set, a SVM classifier is trained to discriminate the final acoustic scene class. Note that the CNN model is a building block in the proposed framework. It can be replaced by any popular CNN architecture, such as ResNet [16], and GoogleNet [17] etc. Moreover, on the basis of the outputs of the basic classifiers, we construct super-class labels for the samples using spectral clustering [24]. These expanded labels are used to improve the basic models by transforming them into multitask learning paradigms. By using these updated models in the feature extraction process, the SVM classifier can be updated accordingly. The contributions of this letter are threefold:

- 1) We propose a multi-spectrogram fusion framework using a single CNN architecture in feature extractions. By aggregating the segment-level features from multiple spectrograms, the proposed framework significantly improves the performance for ASC.
- 2) We propose a novel label expansion method which constructs super-class labels by taking advantage of the similarities in acoustic properties among original classes. The constructed hierarchical labels reflect the relations of the original acoustic scenes from the view of the basic classifiers.
- 3) We use the artificial hierarchical labels to transform the basic CNN-based models into multitask learning architectures. Moreover, the relations between super-class and included original classes are modeled as regularization constrains in the loss function. In this way, the models are guided to extract more essential acoustic features.

II. PROPOSED METHOD

CNN models are usually used in ASC [18] when spectrograms are generated from the audio signal. The spectrogram can be considered as the time-frequency representation of acoustic scene [19], [20]. Since CNN is good at learning spatially local correlations from the input image, it can make good use of the spatial and temporal information in the spectrograms. However, there is a trade-off between frequency and time resolution when producing spectrograms. For some acoustic scene classes with greater temporal recurrent structures, high temporal resolution is more suitable, which requires a smaller frame length. However, some classes prefer

high frequency resolution. The preference of resolution will affect the choice of filter shape in CNN model [21]. On the other hand, the resolution is different on the frequency ranges for different time-frequency representations. For example, Constant-Q-Transform (CQT) captures low and mid-to-low frequencies better than the Mel scale [20]. According to above observations, we propose a single CNN model based fusion framework which extract deep features from multiple spectrograms. As seen in Fig. 1, the framework is composed of four parts, including the generation of multiple spectrograms, the construction of basic CNN models, the boosting of CNN models and the classification based on feature fusion.

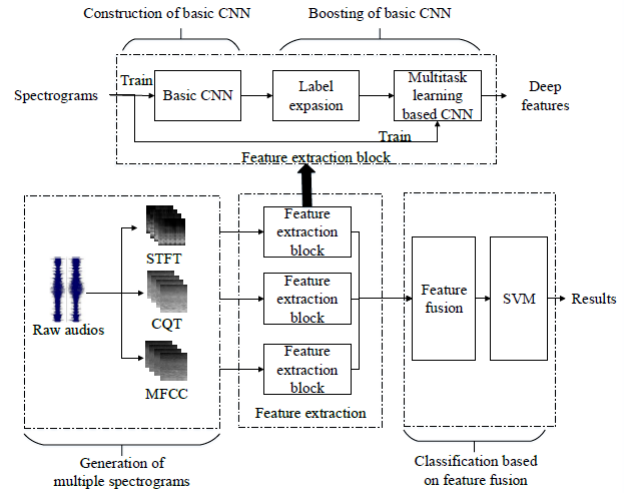


Fig. 1. Framework of the proposed multi-spectrogram fusion model.

III. EXPERIMENTS AND RESULTS

A. Generating STFT, CQT and MFCC spectrograms

STFT, CQT and MFCC spectrograms are applied in this letter. Note that other spectrograms can be adopted as well in our framework. When generating spectrograms, audio signals are divided into frames and frame-level frequency representations are produced using certain transforming techniques. By stacking up the frequency representations frame-by-frame, a corresponding spectrogram is obtained. For STFT spectrogram, we perform Short Time Fourier Transform directly on each audio frame. However, Constant-Q-Transform is used in CQT spectrogram which requires more sampling points on the lower frequency range. For MFCC spectrogram, Mel-filter banks are applied and DCT is performed to get cepstral features. After the spectrograms are ready, they are further split into training/testing samples.

B. Constructing basic CNN models for spectrograms

In our framework, we build up a CNN architecture and train it into multiple classification models. Specifically, we propose a VGG-like network and train it on STFT, CQT and MFCC samples respectively. As a result, three basic CNN models are constructed, namely the VGG-STFT, the VGG-CQT, and the VGG-MFCC models. The architecture of the proposed CNN network is shown in Table I. It was used in our submission to

TABLE I
ARCHITECTURE OF THE PROPOSED CNN NETWORK

Layer	Conv1	Conv2	Pool1	Conv3	Conv4	Pool2	Conv5	Conv6	Conv7	Conv8	Pool3	Conv9	Conv10	Conv11	Full1
Kernel	5×5	3×3	Max, 2×2	3×3	3×3	Max, 2×2	3×3	3×3	3×3	3×3	Max, 2×2	3×3	1×1	1×1	-
Stride	2	1	2	1	1	2	1	1	1	1	2	1	1	1	-
Pad	2	1	0	1	1	0	1	1	1	1	0	0	0	0	-
Channel	32	32	32	64	64	64	128	128	128	128	128	512	512	M*	M*
Activator	ReLu	ReLu	-	ReLu	ReLu	-	ReLu	ReLu	ReLu	ReLu	-	ReLu	ReLu	ReLu	-
BN	Yes	Yes	-	Yes	Yes	-	Yes	Yes	Yes	Yes	-	Yes	Yes	Yes	-
Dropout	-	-	0.3	-	-	0.3	-	-	-	-	0.3	0.5	0.5	-	-

* The variable M represents the number of the output scene classes.

the DCASE2017 challenge [23] and inspired by the one in [3]. To evaluate this network, we compare it with the ResNet in the experiments.

For the better description of the methods, it is necessary to introduce some notations and terminologies. Without loss of generality, the architecture of CNN and the spectrogram are not specified below. Suppose we are given a set of n training samples $S_t = \{(x_1, y_1^o), \dots, (x_n, y_n^o)\}$ with $y_i^o \in \{1, \dots, C\}$ indicating the acoustic scene class label of image x_i (namely a spectrogram patch); superscript o denotes original label of the dataset. For the CNN network, the output layer has C nodes and employs the softmax activation function. Let L be the number of nodes in the next-to-last layer, which is fully connected to the output layer. Let $W_{j,i}$ ($j \in [1, C]; i \in [1, L]$) denote the weights of connections between these two layers. A negative log-likelihood loss is adopted in the basic CNN model, i.e.,

$$L(W) = \frac{1}{n} \sum_{(x_i, y_i^o) \in S_t} (-\log P(y_i^o | x_i, W)) + \alpha \|W\|_2^2 \quad (1)$$

C. Boosting basic CNN models through label expansion

We propose a label expansion method in this letter. For a certain basic CNN model, such as the VGG-STFT, a confusion matrix F can be calculated, with $F_{j,i}$ denotes the number of the samples of class j which are classified as class i by that model. To ensure symmetry of the matrix, F is transformed to a distance matrix D :

$$D = (F + F^T)/2 \quad (2)$$

By applying spectral clustering [24] on the matrix D , we divide the original C classes into N subsets $\{H_1, \dots, H_N\}, H_1 \cup \dots \cup H_N = \{1, \dots, C\}; H_i \cap H_j = \emptyset (i \neq j; i, j \in [1, N])$. Each subset is assigned a super-class label. The label space is expanded by adding N super-class labels into it. Now, every sample has two labels. The S_t can be rewritten as $S_t = \{(x_1, \langle y_1^o, y_1^e \rangle), \dots, (x_n, \langle y_n^o, y_n^e \rangle)\}$ with $y_i^e \in \{1, \dots, N\}$ indicating the super-class label of x_i ; superscript e denotes the expanded label. We have:

$$\forall i \forall j \exists m ((y_i^o \in H_m \wedge y_j^o \in H_m) \rightarrow y_i^e = y_j^e) \quad (3)$$

In this method, the degree of similarity between classes is indicated by the number of misclassification. Samples from the

same super-class are considered as more similar from the view of the basic model. To make the model aware of the inter-class similarities, we add another output layer onto the basic CNN model, leaving all other details of the model unchanged. The newly added layer has N output nodes and is fully connected onto the original next-to-last layer. The weights of the newly added connections are denoted as $U_{(j,i)}$ ($j \in [1, N]; i \in [1, L]$). We then update the reconstruction error of the new model into the type of multitask learning as follows:

$$E = \sum_{((x_i, \langle y_i^o, y_i^e \rangle) \in S_t)} (-\gamma \log P(y_i^o | x_i, W; U) - (1 - \gamma) \log P(y_i^e | x_i, W; U)) \quad (4)$$

Considering that the weight vector $W_j = (W_{j,1}, \dots, W_{j,L})$ for original class j should capture some similar high-level patterns [25], [26] as the weight vector $U_{s(j)} = (U_{s(j),1}, \dots, U_{s(j),L})$ for the super-class $s(j)$ of class j , we introduce the following regularization into the loss function:

$$R = \sum_{j=1}^C \|W_j - U_{s(j)}\|_2^2 \quad (5)$$

Finally, the loss function of the new model can be defined as:

$$L_{LE}(W; U) = E/n + \alpha R + \beta \|W; U\|_2^2 \quad (6)$$

where α and β are set to 0.0001, and γ in Eq. 4 is set to 0.6. After performing this boosting method respectively, we get three new models, namely the VGG-STFT-LE, the VGG-CQT-LE, and the VGG-MFCC-LE models (LE means label expansion is applied).

D. Classifying the acoustic scenes by feature fusion

The new models are used as feature extractors rather than classifiers. For a STFT-spectrogram sample v , given a model, say VGG-STFT-LE, the outputs of activation functions of the next-to-last layer in the model are extracted as its deep features, which is denoted as $f(v)$. As mentioned above, an audio segment g can produce m STFT samples $[v_1^g, \dots, v_m^g]$, which are split from the STFT spectrogram. The subscripts $(1, \dots, m)$ present the occurrence order of the samples within the spectrogram. We feed them into the model and extract their corresponding deep features $f(v_i^g) (i \in [1, m])$. As the time span of a single sample is short, single deep feature

may not depict the whole auditory scene well. To achieve more comprehensive features, they are concatenated into a long feature in random order:

$$O^{STFT}(g) = [f(v_{t1}^g); f(v_{t2}^g); \dots; f(v_{tm}^g)] \quad (7)$$

where $(t1, t2, \dots, tm)$ is a random sequence of numbers 1 to m . To control the risk of overfitting, the principal component analysis (PCA) method is applied to reduce the dimensionality. Eventually, the global feature of STFT-style for audio segment g can be achieved. It is denoted as follows:

$$G^{STFT}(g) = \phi(O^{STFT}(g)) \quad (8)$$

where $\phi()$ means PCA transformation. Likewise, using the CQT and MFCC samples respectively, the global features of $G^{CQT}(g)$ and $G^{MFCC}(g)$ can be obtained as well.

These global features are further fused to generate aggregated features. For example, three kinds of aggregated features can be generated here, which are denoted as $A^{STFT+MFCC}(g)$, $A^{STFT+CQT}(g)$, and $A^{MFCC+CQT}(g)$ respectively. Specifically,

$$A^{(STFT+MFCC)}(g) = [G^{STFT}(g); G^{MFCC}(g)] \quad (9)$$

$$A^{(MFCC+CQT)}(g) = [G^{MFCC}(g); G^{CQT}(g)] \quad (10)$$

$$A^{(STFT+CQT)}(g) = [G^{STFT}(g); G^{CQT}(g)] \quad (11)$$

With these aggregated features, we train SVM classifiers to discriminate the acoustic scenes. Depending on the features used, we can get three SVM classifiers, namely $SVM^{STFT+CQT}$, $SVM^{MFCC+CQT}$, and $SVM^{MFCC+CQT}$ respectively. In our experiments, the $SVM^{STFT+CQT}$ achieves the best performances.

IV. EXPERIMENTS AND RESULTS

A. Experiment Setup

Two widely used benchmark datasets for ASC are selected to evaluate the performances of our methods. The first one is the DCASE2017 dataset¹, which includes two parts, the Development set and the Evaluation set. The second one is the LITIS Rouen dataset [27]².

We generate 16 STFT-spectrogram patches for each audio segment in DCASE2017 dataset and 12 STFT-spectrogram patches for each in LITIS Rouen dataset. The window size is set to 706 and the hop length is 430. When dividing the spectrogram into patches, the width is set to 143 and the shift step is 126. The CQT spectrograms are generated by Librosa 0.5.0 using default settings. For DCASE2017 dataset, 20 CQT patches are produced for each audio segment while 16 patches for each in LITIS Rouen dataset. The width is 143 and shift step is 80 in the CQT patches division process. We use a 180-dim feature to generate MFCC spectrogram. It includes 60 static Mel-frequency cepstral coefficients and their first and second derivatives. When performing transformation, the audio segment is divided into 200-ms frames with a hop length of 100 ms. Again, the MFCC spectrogram is divided into patches by the width of 143 and the shift step of 100.

Consequently, for each audio segment, we generate 20 MFCC patches in DCASE2017 dataset and 30 patches in LITIS Rouen dataset. For all the patches, we resize them into 143*143 before feeding them into the CNN model.

All experiments in this letter are implemented using TensorFlow [28]. During the training of the models, a mini-batch size of 256 is used as well as an early stop strategy with the patience parameter set to 30 and the maximum epoch set to 500. For the VGG-like model, we use Adam [29] as the optimizer with a learning rate of 0.0001. For the ResNet, a momentum optimizer is applied instead, with a learning rate of 0.1 and a momentum of 0.9. In the fusion step, we use the sklearn package in python to implement the PCA and SVM operations. The parameter of n_components is set to 0.99 for keeping 99% information after dimension reduction. For the SVM, the linear kernel is applied and the penalty coefficient is set to 1.

B. Evaluations on DCASE2017 dataset

On the DCASE2017 dataset, we have implemented two set of experiments. One is totally performed on the Development set, evaluated by the 4-fold cross validation (see column Devel-Set in Table II). The other one is trained on the Development set and tested on the Evaluation set (see column Eval-Set in Table II). We have generated STFT, CQT and MFCC spectrograms and trained basic classification models respectively. To evaluate our methods, we also use ResNet-50 to build up basic models besides the proposed VGG-like architecture. For each model, we provide two accuracies: one is the sample-level average accuracy and the other is the segment-level majority voting accuracy.

As shown in Table II, for the Development set, the best sample-level accuracy is 0.7582; the best voting accuracy is 0.8336, both achieved by the VGG-STFT-LE model. For the Evaluation set, the best sample-level accuracy is 0.5921 by ResNet-CQT-LE, however, the best voting accuracy is 0.684, achieved by ResNet-CQT. From Table II, we can see that all voting accuracies significantly outperform the corresponding sample-level ones. The VGG-like is better in the Development set while the ResNet wins in the Evaluation set. For almost all cases, the performances are improved when label expansion is applied, except the voting accuracy of ResNet-CQT-LE on the Evaluation set. Table III has shown the superiorities of multi-spectrogram fusions. The best accuracy for the Development set is improved from 0.8336 to 0.8865. Meanwhile, the one for the Evaluation set is improved from 0.6840 to 0.7778. The fusions of STFT and CQT achieve the best results for all the models and both datasets. Their fusions can obviously improve the accuracies. Although the best result for Development set is achieved by VGG-LE with STFT+CQT features, ResNet-LE has won in all other cases. Therefore, ResNet is more suitable for DCASE2017. Finally, label expansion is indeed helpful here. It improves the performances for both models with all aggregated features.

C. Evaluations on LITIS Rouen dataset

We also evaluate our methods on the LITIS Rouen dataset. When using single spectrogram, the best sample-

¹<http://www.cs.tut.fi/sgn/arg/dcase2017/challenge/download>

²<https://sites.google.com/site/alainrakotomamonjy/home/audio-scene>

TABLE II
CLASSIFICATION PERFORMANCES ON THE DCASE2017 DATASETS USING
DIFFERENT SINGLE SPECTROGRAM.

Model	Devel-Set		Eval-Set	
	Sample-Level	Voting	Sample-Level	Voting
VGG-STFT	0.7274	0.8056	0.4562	0.5296
VGG-STFT-LE	0.7582	0.8336	0.5356	0.6494
VGG-CQT	0.7255	0.8159	0.5576	0.6432
VGG-CQT-LE	0.7404	0.8199	0.5859	0.6735
VGG-MFCC	0.6451	0.7649	0.4571	0.5673
VGG-MFCC-LE	0.6461	0.7685	0.4771	0.5938
ResNet-STFT	0.7374	0.817	0.5248	0.6123
ResNet-STFT-LE	0.745	0.8176	0.5456	0.6525
ResNet-CQT	0.7221	0.8039	0.588	0.684
ResNet-CQT-LE	0.7365	0.8257	0.5921	0.6796
ResNet-MFCC	0.6553	0.7766	0.476	0.584
ResNet-MFCC-LE	0.6675	0.7994	0.4866	0.6142

TABLE III
CLASSIFICATION PERFORMANCES ON THE DCASE2017 DATASETS
US-ING MULTI-SPECTROGRAM FUSION.

Dataset	Aggregated Features	VGG	VGG-LE	ResNet	ResNet-LE
Devel-Set	STFT+CQT	0.8756	0.8865	0.8773	0.8852
Devel-Set	STFT+MFCC	0.85	0.8592	0.8568	0.8747
Devel-Set	MFCC+CQT	0.8364	0.8478	0.8508	0.8545
Eval-Set	STFT+CQT	0.6914	0.7302	0.7654	0.7778
Eval-Set	STFT+MFCC	0.6778	0.6988	0.7234	0.7321
Eval-Set	MFCC+CQT	0.6222	0.6728	0.6907	0.6957

level accuracy and segment-level accuracy are 0.8901 and 0.9614 respectively, both achieved by ResNet-CQT-LE, as shown in Table IV. Table V demonstrates the results of the multi-spectrogram fusions. With the aggregated features of STFT+CQT, the accuracies on the four models (VGG, VGG-LE, ResNet, ResNet-LE) are all above 0.97, outperforming the ones of all other aggregated features. The highest one obtained by the aggregated features of STFT+CQT is 0.9744, which is an improvement of 0.013 over the best accuracy using single spectrogram (i.e., 0.9614). It has again validated the effectiveness of the multi-spectrogram fusion. Moreover, our best accuracy has been very close to the current state-of-the-art accuracy (0.978) achieved in [30]. It should be mentioned that no all fusions can improve the performances here. For example, the accuracies with the fusions of STFT+MFCC and MFCC+CQT are both less than 0.9614. These declines in accuracies have illustrated the importance of aggregated feature selection. For the comparison of basic models, there is no prevailing model for all aggregated features. In detail, for the aggregated features of STFT+CQT, the best basic model is ResNet, while the VGG-like models are better for the other two aggregated features.

TABLE IV
CLASSIFICATION PERFORMANCES ON THE LITIS ROUEN DATASET USING
DIFFERENT SINGLE SPECTROGRAM.

Model	Sample-Level	Voting
VGG-STFT	0.8504	0.9451
VGG-STFT-LE	0.8566	0.9482
VGG-CQT	0.8735	0.9564
VGG-CQT-LE	0.8748	0.956
VGG-MFCC	0.7114	0.9077
VGG-MFCC-LE	0.7145	0.9117
ResNet-STFT	0.8671	0.9458
ResNet-STFT-LE	0.8687	0.947
ResNet-CQT	0.8895	0.9588
ResNet-CQT-LE	0.8901	0.9614
ResNet-MFCC	0.7201	0.9051
ResNet-MFCC-LE	0.7113	0.8997

TABLE V
CLASSIFICATION PERFORMANCES ON THE LITIS ROUEN DATASET USING
MULTI-SPECTROGRAM FUSION.

Aggregated Features	VGG	VGG-LE	ResNet	ResNet-LE
STFT + CQT	0.9703	0.9707	0.9744	0.9738
STFT + MFCC	0.9502	0.9486	0.943	0.9476
MFCC+CQT	0.9591	0.9555	0.9589	0.9586

As shown in the Table V, label expansion does not always work in the LITIS Rouen dataset. First, even it helps, the improvement gained is slight. Second, the accuracy would slightly decrease in some cases when it is applied. For example, with the aggregated features of STFT+CQT, the accuracy achieved by ResNet-LE is 0.9738 versus 0.9744 by ResNet. However, label expansion is found really work in DCASE2017 dataset. We suppose that the difference lies in the distributing characteristics of the datasets. When the clustered subsets in the dataset are separable, label expansion will play an effective role. On the contrary, it will fail when the boundaries of the subsets are ambiguous. To further testify its usefulness, we conduct experiments on another environmental sound dataset of ESC-50 [31]. Using the aggregated features of STFT+CQT, the accuracy achieved by VGG is 0.7145 versus 0.7285 by VGG-LE. An improvement of 0.014 is gained by label expansion, which has proven its effectiveness.

V. CONCLUSION

In this letter, we have proposed a CNN-based multi-spectrogram fusion framework for acoustic scene classification. The fusion of STFT and CQT spectrograms achieves the best performance for all datasets and CNN models in our experiments. Motivated by the inter-class similarities in the datasets, a label expansion method is proposed where super-class labels are constructed. The super-class labels are

TABLE VI
ACCURACY COMPARISON OF DIFFERENT METHODS.

Method	DCASE2017 Develop- ment Set	DCASE2017 Evaluation Set	LITIS Rouen Dataset
RNN- Fusion [32]	-	-	0.978
CNN- Fusion6 [32]	-	-	0.966
Scene+Speech- LTE [33]	-	-	0.964
FisherHOG+ ProbSVM [34]	-	-	0.96
CNN-LSTM- GAN [7]	0.871	0.833 ³	-
Background Subtrac- tion [35]	0.919	0.804 ³	-
Mixup Multi- Channel [36]	0.872	0.767	-
Multi-temporal Resolution [37]	-	0.747	-
LEW score fu- sion [38]	0.887	0.741	-
Scalogram- CNN- GRNN [9]	0.844	0.64	-
Our method	0.8865	0.7778	0.9744

utilized to transform the CNN model into multitask learning paradigm. Moreover, the relations between the super-classes and the original scene classes are modeled as regularization constrains in the loss function. Label expansion takes effect on some datasets, depending on the distributing characteristics of the datasets. Generally, the proposed methods have achieved promising results on both the DCASE2017 and the LITIS Rouen datasets.

REFERENCES

- [1] D. Barchiesi, D. Giannoulis, S. Dan, and M. D. Plumbley, "Acoustic scene classification: Classifying environments from the sounds they produce," *IEEE Signal Processing Magazine*, vol. 32, no. 3, pp. 16–34, 2015.
- [2] D. Yu and J. Li, "Recent progresses in deep learning based acoustic models," *IEEE/CAA Journal of Automatica Sinica*, vol. 4, no. 3, pp. 396–409, 2017.
- [3] H. Eghbal-Zadeh, B. Lehner, M. Dorfer, and G. Widmer, "Cp-jku submissions for dcase-2016: a hybrid approach using binaural i-vectors and deep convolutional neural networks," 2016.
- [4] N. Dehak, P. J. Kenny, R. Dehak, P. Dumouchel, and P. Ouellet, "Front-end factor analysis for speaker verification," *IEEE Transactions on Audio Speech & Language Processing*, vol. 19, no. 4, pp. 788–798, 2011.
- [5] S. H. Bae, I. Choi, and N. S. Kim, "Acoustic scene classification using parallel combination of LSTM and CNN," 2016.
- [6] A. Graves, "Long short-term memory," *Neural Computation*, vol. 9, no. 8, pp. 1735–1780, 1997.
- [7] S. Mun, S. Park, D. K. Han, and H. Ko, "Generative adversarial network based acoustic scene training set augmentation and selection using svm hyper-plane," *Proc. DCASE*, pp. 93–97, 2017.
- [8] I. J. Goodfellow, J. Pouget-Abadie, M. Mirza, B. Xu, D. Warde-Farley, S. Ozair, A. Courville, and Y. Bengio, "Generative adversarial networks," *Advances in Neural Information Processing Systems*, vol. 3, pp. 2672–2680, 2014.
- [9] Z. Ren, K. Qian, Z. Zhang, V. Pandit, A. Baird, and B. Schuller, "Deep scalogram representations for acoustic scene classification," *IEEE/CAA Journal of Automatica Sinica*, vol. 5, no. 3, 2018.
- [10] J. Chung, C. Gulcehre, K. H. Cho, and Y. Bengio, "Empirical evaluation of gated recurrent neural networks on sequence modeling," *Eprint Arxiv*, 2014.
- [11] X. Zhang, F. Zhou, Y. Lin, and S. Zhang, "Embedding label structures for fine-grained feature representation," in *IEEE Conference on Computer Vision and Pattern Recognition*, 2016, pp. 1114–1123.
- [12] Z. Han, B. Wei, Y. Zheng, Y. Yin, K. Li, and S. Li, "Breast cancer multi-classification from histopathological images with structured deep learning model," *Scientific Reports*, vol. 7, no. 1, p. 4172, 2017.
- [13] S. H. Nawab, "Short-time fourier transform," in *Advanced Topics in Signal Processing*, 1988, pp. 289–337.
- [14] J. C. Brown and M. S. Puckette, "An efficient algorithm for the calculation of a constant q transform," *Journal of the Acoustical Society of America*, vol. 92, no. 5, p. 2698, 1992.
- [15] B. Logan, "Mel frequency cepstral coefficients for music modeling," *Proc of Ismir*, 2000.
- [16] K. He, X. Zhang, S. Ren, and J. Sun, "Deep residual learning for image recognition," pp. 770–778, 2015.
- [17] C. Szegedy, W. Liu, Y. Jia, P. Sermanet, S. Reed, D. Anguelov, D. Erhan, V. Vanhoucke, and A. Rabinovich, "Going deeper with convolutions," pp. 1–9, 2014.
- [18] S. Hershey, S. Chaudhuri, D. P. W. Ellis, J. F. Gemmeke, A. Jansen, R. C. Moore, M. Plakal, D. Platt, R. A. Saurous, and B. Seybold, "Cnn architectures for large-scale audio classification," in *IEEE International Conference on Acoustics, Speech and Signal Processing*, 2017, pp. 131–135.
- [19] E. Sejdi, I. Djurovi, and J. Jiang, *Time-frequency feature representation using energy concentration: An overview of recent advances*. Academic Press, Inc., 2009.
- [20] B. Boashash, N. A. Khan, and T. Ben-Jabeur, *Time-frequency features for pattern recognition using high-resolution TFDs*. Academic Press, Inc., 2015.
- [21] D. Battaglino, "Acoustic scene classification using convolutional neural networks," 2016.
- [22] T. Lidy and A. Schindler, "Cqt-based convolutional neural networks for audio scene classification," in *Detection and Classification of Acoustic Scenes and Events 2016 Workshop*, 2016.
- [23] Z. Weiping, Y. Jiantao, X. Xiaotao, L. Xiangtao, and P. Shaohu, "Acoustic scene classification using deep convolutional neural network and multiple spectrograms fusion," in *Detection and Classification of Acoustic Scenes and Events 2017 Workshop (DCASE2017)*, 2017.
- [24] A. Y. Ng, M. I. Jordan, and Y. Weiss, "On spectral clustering: analysis and an algorithm," *Proc Nips*, vol. 14, pp. 849–856, 2001.
- [25] S. Xie, T. Yang, X. Wang, and Y. Lin, "Hyper-class augmented and regularized deep learning for fine-grained image classification," in *IEEE Conference on Computer Vision and Pattern Recognition*, 2015, pp. 2645–2654.

- [26] S. Gopal and Y. Yang, "Recursive regularization for large-scale classification with hierarchical and graphical dependencies," in *ACM SIGKDD International Conference on Knowledge Discovery and Data Mining*, 2013, pp. 257–265.
- [27] A. Rakotomamonjy and G. Gasso, "Histogram of gradients of time-frequency representations for audio scene classification," *IEEE/ACM Transactions on Audio Speech & Language Processing*, vol. 23, no. 1, pp. 142–153, 2017.
- [28] M. Abadi, A. Agarwal, P. Barham, E. Brevdo, Z. Chen, C. Citro, G. S. Corrado, A. Davis, J. Dean, and M. Devin, "Tensorflow: Large-scale machine learning on heterogeneous distributed systems," 2015.
- [29] D. Kingma and J. Ba, "Adam: A method for stochastic optimization," *Computer Science*, 2014.
- [30] H. Phan, P. Koch, F. Katzberg, M. Maass, R. Mazur, and A. Mertins, "Audio scene classification with deep recurrent neural networks," 2017.
- [31] K. J. Piczak, "Esc: Dataset for environmental sound classification," in *ACM International Conference on Multimedia*, 2015, pp. 1015–1018.
- [32] H. Phan, L. Hertel, M. Maass, P. Koch, R. Mazur, and A. Mertins, "Improved audio scene classification based on label-tree embeddings and convolutional neural networks," *IEEE/ACM Transactions on Audio Speech & Language Processing*, vol. 25, no. 6, pp. 1278–1290, 2017.
- [33] H. Phan, L. Hertel, M. Maass, P. Koch, and A. Mertins, "Label tree embeddings for acoustic scene classification," in *ACM on Multimedia Conference*, 2016, pp. 486–490.
- [34] J. Ye, T. Kobayashi, M. Murakawa, and T. Higuchi, "Acoustic scene classification based on sound textures and events," in *ACM International Conference on Multimedia*, 2015, pp. 1291–1294.
- [35] Y. Han, J. Park, and K. Lee, "Convolutional neural networks with binaural representations and background subtraction for acoustic scene classification," in *Detection and Classification of Acoustic Scenes and Events*, 2017.
- [36] K. Xu, D. Feng, H. Mi, B. Zhu, D. Wang, L. Zhang, H. Cai, and S. Liu, "Mixup-based acoustic scene classification using multi-channel convolutional neural network," 2018.
- [37] B. Zhu, K. Xu, D. Wang, L. Zhang, B. Li, and Y. Peng, "Environmental sound classification based on multi-temporal resolution convolutional neural network combining with multi-level features," 2018.
- [38] R. Hyder, S. Ghaffaradegan, Z. Feng, and T. Hasan, "Buet bosch consortium (b2c) acoustic scene classification systems for dcase 2017 challenge."